

Ultrafast Ring Closure Energetics and Dynamics of Cyclopentadienyl Manganese Tricarbonyl Derivatives

Tianjie Jiao, Zhen Pang,¹ Theodore J. Burkey*

The Department of Chemistry, Campus Box 526060
The University of Memphis
Memphis, Tennessee 38152-6060
voice: 901-678-2634
Telefax: 901-678-3447
e-mail: tburkey@memphis.edu

Randy F. Johnston

Department of Chemistry
Union University
Jackson, Tennessee 38305

Todd A. Heimer,² Valeria D. Kleiman³ and Edwin J. Heilweil*

B208 Building 221, Physics Laboratory
National Institute of Standards and Technology
Gaithersburg, MD 20899
voice: 301-975-2370
e-mail: edwin.heilweil@nist.gov

¹ Current Address, Department of Chemistry, Fudan University, China

² NIST/NRC Postdoctoral Associate

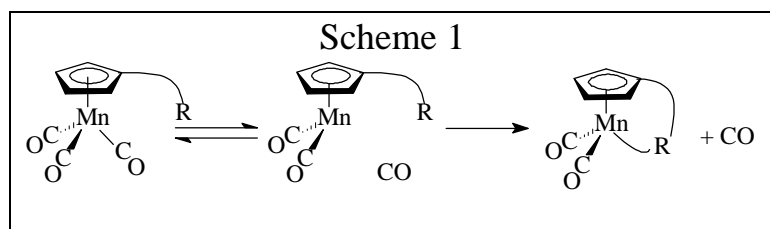
³ Guest Researcher from UCLA Department of Chemical Engineering. Current address: Condensed Matter and Radiation Sciences Division, Naval Research Laboratory, Washington, DC 20375

Abstract

Ring closure following flash photolysis in alkane solvents has been detected for several complexes in the series $(\eta^5\text{-C}_5\text{H}_4\text{R})\text{Mn}(\text{CO})_3$ where $\text{R} = \text{COCH}_3$ (**1**), $\text{COCH}_2\text{SCH}_3$ (**2**), $\text{CO}(\text{CH}_2)_2\text{SCH}_3$ (**3**), $\text{COCH}_2\text{OCH}_3$ (**4**), $(\text{CH}_2)_2\text{CO}_2\text{CH}_3$ (**5**), $\text{CH}_2\text{CO}_2\text{CH}_3$ (**6**). Photoacoustic calorimetry studies reveal that ring closures occur with rate constants faster than 10^7 s^{-1} or between 10^6 - 10^7 s^{-1} , or in some cases the ring closure is biphasic with rate constants in both ranges. The enthalpies for ring closure of **2** and **3** are the same (12 kcal/mol) and less favorable than those for **4-6** (25-15 kcal/mol). Studies of **1-3** by transient ps to μs infrared spectroscopy further indicate biphasic dynamics for **2** and **3**: ring closure occurs immediately ($k > 5 \times 10^9 \text{ s}^{-1}$) and at slower rates ($k = 10^8 - 10^6 \text{ s}^{-1}$). The ultrafast ring closure appears to be as fast or faster than solvent coordination, which is also observed to occur. The relationships of the rates and energetics of ring closure to structure and quantum yields are discussed.

Introduction

The yields of products generated from photolytic fragments can be dependent on geminate recombination or interactions with the solvent,^{1,2} which often occur faster than diffusion-controlled processes.³ In such cases efforts to change quantum yields require intervention at very short time scales. We recently succeeded in dramatically improving the quantum yields for the ligand



substitution of $(C_5H_4R)Mn(CO)_3$ complexes by providing side chains that could effectively trap the coordinatively-unsaturated metal center

(Scheme 1).⁴ In particular, unit quantum yields for ring closure were observed in at least two cases, and require that CO recombination does not occur. The latter process has been reported to have a lifetime on the order of 300 fs for other metal carbonyls.³ This suggests that ring closure must occur in less than 300 fs, a lifetime much shorter than those typically reported for closure of 5-6 membered rings.^{5,6} In this study, we have investigated the dynamics and energetics of ring closure of $(C_5H_4R)Mn(CO)_3$ by using photoacoustic calorimetry (PAC) and transient infrared spectroscopy to better understand how the side-chain structure effects the quantum yield for substitution.

Experimental Section

All materials were obtained from Sigma-Aldrich and used without further purification unless otherwise stated.⁷ Heptane was refluxed over sodium under argon for several hours before distillation. Tetrahydrothiophene (THT) was distilled after refluxing over calcium hydride. Ferrocene was sublimed under vacuum. Tetrahydrofuran was distilled from sodium-potassium alloy. The synthesis of $(\eta^5-C_5H_4R)Mn(CO)_3$ derivatives have been reported previously,^{8,9} although better

procedures for synthesizing **2** and **3** are reported in the Supplementary Material. All measurements were conducted at room temperature, and metal carbonyls used in transient infrared experiments were dissolved in *n*-hexane (Fisher Optima grade) without any further purification or degassing. The error limits of heat amplitudes and rate constants from PAC studies are reported as 1σ . The error limits of rate constants from transient infrared studies are reported as 1σ or 10%, whichever is greater.

(1-ethanoyl)cyclopentadienyl manganese tetrahydrothiophene dicarbonyl. A 250-mL cyclohexane solution containing tetrahydrothiophene (2.18 g, 24.7 mmol) and **1** (0.20 g, 0.81 mmol) was placed in an immersion well and irradiated by 300 nm lamps in a Rayonet reactor for 50 min. The solution was filtered through a celite pad. The residue, after evaporation, was eluted from a silica column with 5% ethyl acetate in benzene. Upon evaporation of solvent a red-brown liquid was obtained (0.174g, 70 %). Found: C, 51.85; H, 4.90; Mn, 17.78; S, 9.99; calcd. ($C_{13}H_{15}MnO_3S$): C, 50.95; H, 4.94; Mn, 17.94; S, 10.47. IR (cyclohexane) 1944 (vs), 1885 (vs), and 1674 (m) cm^{-1} ; 1H NMR (270 MHz, $CDCl_3$) δ 5.01 (t, $J = 2.25$ Hz, 2 H), 4.54 (t, $J = 2.25$ Hz, 2 H), 2.73 (m, 4 H) 2.33 (s, 3 H) 1.96 (m, 4H); ^{13}C NMR (67.5 MHz, $CDCl_3$) δ 231.5, 198.2, 89.5, 87.9, 81.2, 43.6, 30.2, 26.9.

Photoacoustic Calorimetry. The apparatus and methods have been described previously.^{10,11} A solution irradiated with a laser pulse in a flow cell produces an acoustic wave that is detected as a signal from an ultrasonic transducer clamped to the cell. Ferrocene was used in a reference solution to provide an instrument limited signal (*ca.* 0.1 μs).¹² Samples signals were deconvoluted with the ferrocene signal by using MQP or Sound Analysis 3000 by Quantum Northwest. The deconvolution software expresses the amplitude of the sample heat decays (ϕ) as a fraction of the heat deposited by the reference solution. One or two heat decays were detected in each case. The amplitude of the first heat decay (ϕ_1) corresponds to those processes with lifetimes (τ_1) much faster than the transducer response. Heat decays for these processes cannot be resolved from each other. The amplitude of the

second heat decay (ϕ_2) corresponds to processes evolving heat with lifetimes (τ_2) comparable to the transducer response. The enthalpy per mole of absorbed photons and rate constants were calculated from eq 1-3 where E_{hv} is the photon energy.

$$\Delta H_1 = E_{\text{hv}}(1 - \phi_1)/\Phi \quad (1)$$

$$\Delta H_2 = -E_{\text{hv}}\phi_2/\Phi \quad (2)$$

$$1/\tau_2 = k_0 + k_2[\text{L}] \quad (3)$$

In a typical experiment, **1** (5.9 mg, 24 μmol) was dissolved in 50 mL of heptane in a glove box. This solution (31.8 mL) was diluted to 200 mL with heptane to make a 0.1 OD (optical density) at 337 nm. The dilute solution was cannulated into a calibrated helium-purged reservoir with triethylphosphate (740 μL , 4.4 mmol) to a final volume of 50 mL. The maximum laser energy was 20 μJ /pulse at 337 nm. The laser was pulsed at one Hz, and PAC signals were not used if pulse energies varied more than 1 μJ from an average value. Sample solutions were passed through a flow cell so that exposed solution would not be irradiated by a subsequent pulse. Signals from 1 or 0.1 Mhz transducers were averaged for 16-32 shots. The values of ϕ_1 , ϕ_2 , and τ_2 did not change when the pulse energy was decreased by three-fold. Ligand concentrations were varied by at least ten-fold.

Transient Infrared Spectroscopy.

Ultrafast infrared spectroscopy was performed using the NIST picosecond apparatus described in detail earlier.¹³ Modifications to the pulse compressed, regeneratively amplified (20 Hz), synchronously pumped, dual dye (R6G, DCM) laser system were made for broadband, multichannel probing and transient detection using an InSb 256x256 infrared array camera system.¹⁴ Time delays (ps-ns) were obtained with a computer-controlled optical delay stage, and UV excitation was performed at 289 nm (doubled R6G laser, 2 ps instrument resolution). All measurements were made using a flowing 1 mm path-length cell with CaF_2 windows, and solute concentrations in *n*-

hexane were varied (typically 2-4 mM) to yield UV optical densities near 1.0. Transient difference spectra spanning approximately 100 cm^{-1} centered around 1960 cm^{-1} were obtained by iteratively collecting probe and reference spectra with the pump on and off (4000 total laser shots) and then averaging up to five difference spectra to produce a final averaged spectrum at each time delay. Kinetic data and transient lifetimes were obtained by fitting peak intensities as a function of time delay for spectral bands that did not overlap with other IR bands.

An electronically delayed, Q-switched excitation laser (5 ns, 266 nm, 250 μJ at 20 Hz) was employed for >5 ns time domain measurements. This laser was synchronized to the ps probe laser and array detection systems with a digital delay generator (Stanford Research Systems 535) which provided output triggers for the lamp, Q-switch and InSb array controller. These pulses were synchronously delayed (up to *ca.* 25 ms) from the ps laser system master clock (20 Hz TTL count-down signals obtained from the 41 MHz acousto-optic RF oscillator). Pump-probe delay timing was adjusted by monitoring a fast photodiode which measured pump and visible probe scatter from the sample cell front window. In this fashion, pump-probe time delays could be selected spanning ns to μs (probe arrival before or after pump), and jitter between the pump and probe pulses was determined to be less than 1 ns. While this approach is somewhat unconventional, the method provides ps to ms time-delayed transient mid-IR spectra with mOD sensitivity, covering over 100 cm^{-1} in about 10 minutes (*ca.* 4000 laser shots).

Note that different excitation wavelengths were used in the PAC and transient experiments. Steady state photolysis at various wavelengths (150W Xe lamp / monochrometer source) revealed that the FTIR spectrum and quantum yield of the photoproduct are independent of excitation wavelengths in the range of 290–330 nm.

Molecular Mechanics. The conformational energies of **2** and **3** were optimized by using CAChe.

Dihedral angles were incremented every 15 degrees while the potential energy of the whole molecule was optimized. Conformations about two bonds were examined for **2**: the bond between the first ethanoyl carbon and the cyclopentadienyl ring carbon and the bond between the first and second carbons of the ethanoyl group. Conformations about three bonds were examined for **3**: the bond between the first propanoyl carbon and the cyclopentadienyl ring, the bond between the first and second propanoyls carbons, and the bond between the second and third propanoyl carbons.

Results

Our studies began with PAC studies of **1** where the displacement of CO by solvent could be observed with negligible competition from dispersed ligands (THF, THT, and triethylphosphate) or ring closure. As expected only a single heat decay (ϕ_1) was detected for **1** in the absence of dispersed ligands. When a dispersed ligand was present with **1** the rate constant of the second heat decay increased with increasing ligand concentration (Figure 1). The amplitudes of the heat decays for **1** were dependent on the dispersed ligand concentration although the sum of the amplitudes was not (Figure 2). The ϕ_1 and ϕ_2 values were extrapolated to zero ligand concentration for the data reported in Table 1. At higher

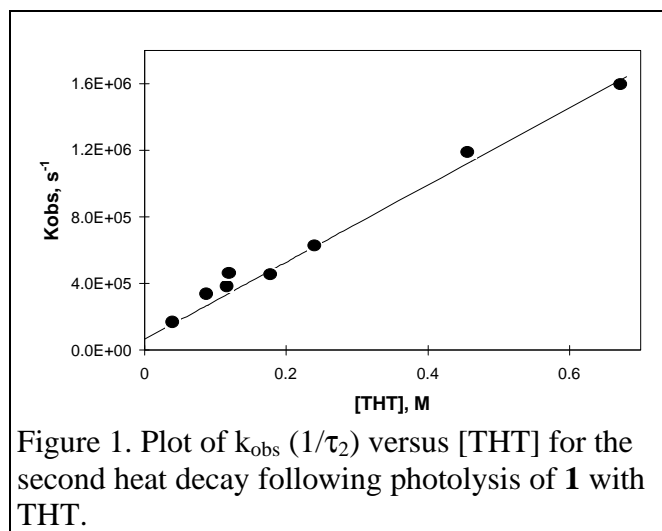


Figure 1. Plot of k_{obs} ($1/\tau_2$) versus $[\text{THT}]$ for the second heat decay following photolysis of **1** with THT.

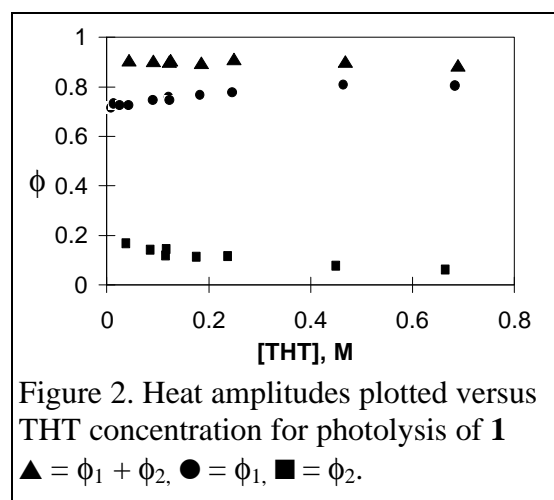


Figure 2. Heat amplitudes plotted versus THT concentration for photolysis of **1**
▲ = $\phi_1 + \phi_2$, ● = ϕ_1 , ■ = ϕ_2 .

concentrations of $\text{OP}(\text{OEt})_3$, saturation was observed in the kinetic data, so the rate constant was obtained from the linear portion of the data.

Transient IR experiments reveal that photolysis of **1** with 0.36 M THT in *n*-hexane produces transient and product bands. The photolysis results in an initial bleach of the 1961 and 1952 cm^{-1} bands for **1**, and the amplitude of the bleach did not change during the remainder of the experiment. Two transient bands (**1A**) appear at 1907 and 1969 cm^{-1} within the first 200 ps after excitation.¹⁵ The

transient bands of **1A** decay with the same rate as two new absorption bands of **1B** grow at 1946 and 1885 cm^{-1} . The **1B** bands are stable indefinitely (monitored up to 10 μs delay). Similar results were observed following photolysis of **2** or **3** in the absence of THT, except that partial appearance of the product bands was also observed within 200 ps. For example, as shown in Figure 3, upon photolysis of **2**, there is a bleach (peaks below baseline) of parent bands at 1962 and 1953 cm^{-1} and the immediate appearance of bands at 1968, 1958, 1906 and 1898 cm^{-1} . The 1968 and 1906 cm^{-1} band intensities (**2A**) decay as the 1958 and 1898 cm^{-1} band intensities (**2B**) grow. At μs time delays

when the 1906 cm^{-1} band of **2A** has disappeared, the intensity of the 1898 cm^{-1} band of **2B** is equal to the sum of the intensities of the 1898 and 1906 cm^{-1} bands at earlier delays. No other CO stretch IR bands are observed in this frequency range. The spectra and intensities of analogous bands for **1** and

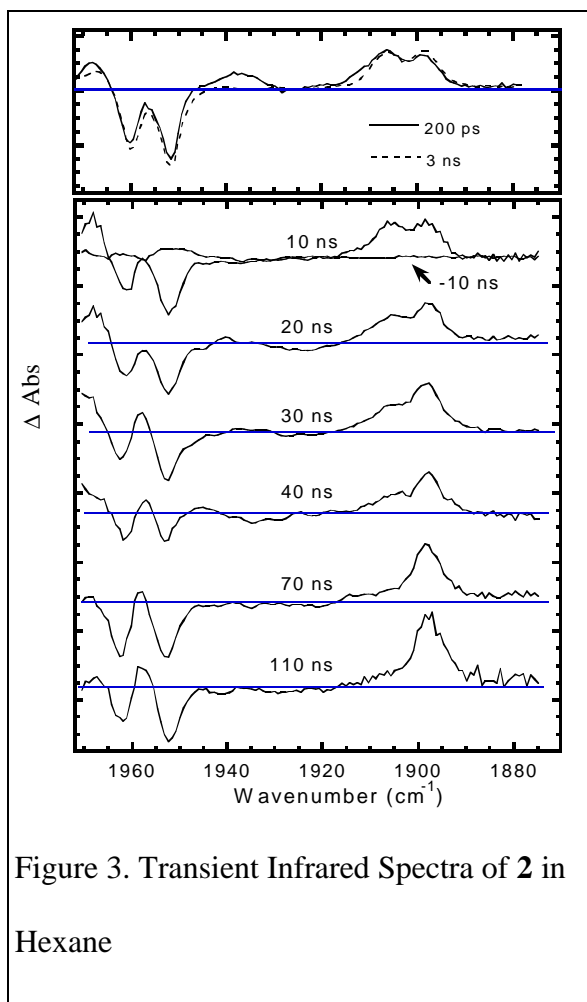


Figure 3. Transient Infrared Spectra of **2** in Hexane

3 behaved similarly. All derived spectral and kinetic data for transients from similar transient spectra of the other systems are summarized in Table 2.

Table 1. PAC Data for Photolysis of (η^5 -C₅H₄R)Mn(CO)₃ in Heptane

complex n	Φ^a	ϕ_1	ϕ_2	DH_1	DH_2	$DH_1 + DH_2$	$10^{-6}k^b$
kcal/mol							
1 (+ THT)	0.82	0.714 \pm 0.007	0.185 \pm 0.019	29.6 \pm 1.9	-19.1 \pm 1.2	10.5 \pm 2.5	2.3 \pm 0.1
1 (+ THF)	0.82	0.710 \pm 0.023	0.090 \pm 0.008	30.0 \pm 3.0	-9.3 \pm 1.0	20.7 \pm 3.2	0.20 \pm 0.04
1 + OP(OEt) ₃		0.703 \pm 0.015	0.159 \pm 0.023	30.7 \pm 2.4	-16.4 \pm 2.6	14.3 \pm 3.5	5.3 \pm 2.8
2	1.00	0.862 \pm 0.030	^c	11.7 \pm 2.6	^c	11.7 \pm 2.6	^c
3	0.82	0.785 \pm 0.014	0.098 \pm 0.007	22.2 \pm 2.0	-10.0 \pm 1.0	12.2 \pm 2.2	1.14 \pm 0.10 ^d
4	0.64	0.718 \pm 0.014	0.044 \pm 0.006	37.4 \pm 3.5	-5.8 \pm 0.9	31.6 \pm 3.6	0.97 \pm 0.13 ^d
4	(0.82) ^e			29.2 \pm 2.3	-4.6 \pm 0.7	24.6 \pm 2.4	
5	1.05	0.718 \pm 0.013	0.081 \pm 0.010	22.8 \pm 1.7	-6.5 \pm 0.9	16.3 \pm 1.9	4.6 \pm 0.5 ^d
6	0.94 ^f	0.782 \pm 0.010	0.016 \pm 0.006	19.7 \pm 1.4	-1.4 \pm 0.5	15.2 \pm 1.6	0.8 \pm 0.4 ^d

^afrom reference 4, ^bunits are M⁻¹ s⁻¹ unless otherwise noted, ^cnot detected, ^dunits are s⁻¹, ^esee Discussion, ^ftotal yield for all photoproducts, see reference 4

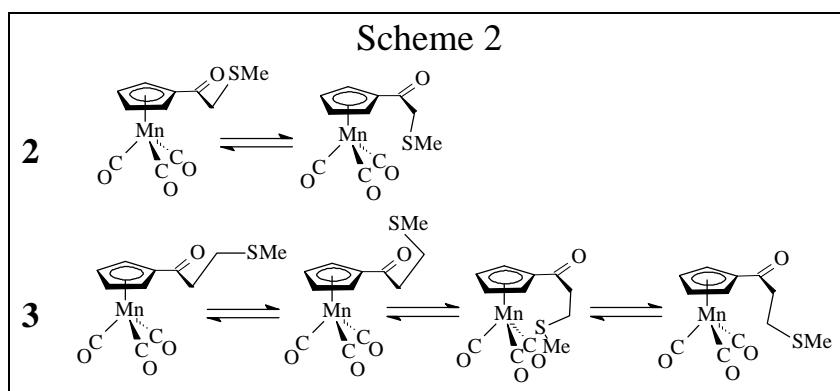
Table 2. Transient IR following Photolysis of (C₅H₄R)Mn(CO)₃ in *n*-hexane

IR after 266 nm photolysis ^a					200 ps	10 ⁻⁶ k _{obs} s ⁻¹	
complex n	nA		nB		[nB]/[nA]	nA	nB
1 ^b	<u>1907</u>	1969	<u>1946</u>	1885	0	2.3±0.6	2.7±0.7
2	<u>1906</u>	1968	1958	1898	1	29±10	^c
3	1907	1968	1958	1895	0.3	3.8±0.8	4.3±1.6

^a(\pm 3 cm⁻¹), underlined bands were used for kinetic analysis, **A** is the transient and **B** is the product, see Schemes 3 and 4, ^b0.36 M THT, ^cnot determined

Molecular mechanics calculations show that there is a considerable barrier (*ca.* 6 Kcal/mol) to the rotation about the carbonyl carbon of the side chain and the cyclopentadienyl ring for both **2** and **3**. Thus the side chain carbonyls stay in the plane of the cyclopentadienyl ring. Only half of the conformations are discussed and displayed in Scheme 2 since an identical set of conformations occur when the side chain carbonyls are rotated 180°. Two conformations of nearly equal energy were found for **2** where the thiomethyl group is above or below the plane of the ring. Four conformations

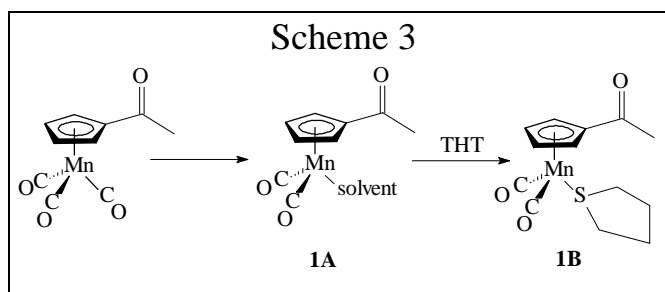
of nearly equal energy were found for **3**, and only one of these conformations has the thiomethyl group in the proximity of the metal center.



Discussion

The results indicate that **2-6** undergo ring closure following photolysis. It is clear that in some cases, if not all, ring closure is biphasic. First, following CO dissociation there is an immediate ring closure that competes with solvent coordination. Second, the fraction of compound that has not immediately ring-closed does so by displacing the solvent. This sequence is best understood by first examining **1** where ring closure was not observed.

The second heat decay observed after photolysis of **1** is assigned to the reaction of **1A** with THT (Scheme 3, second step). The ΔH_2 calculated from the ϕ_2 for this reaction is exothermic; a result that is expected for a process where the bond formed (Mn-S) is stronger than the bond broken (Mn-heptane). In addition this assignment is consistent with (a) the dependence of the observed rate constant for ϕ_2 on THT concentration (Figure 1), (b) the change in ϕ_2



concentration (Figure 1), (b) the change in ϕ_2 with ligand structure (see Table 1) and (c) the observed changes in the IR spectra (Table 2).¹⁶ In particular, the 1907 and 1969 cm^{-1} bands (which decay) are assigned to **1A** by a comparison with the bands observed for $(\text{C}_5\text{H}_5)\text{Mn}(\text{CO})_2(\text{heptane})$ (1895 and 1964 cm^{-1}),¹⁷ and the 1946 and 1885 cm^{-1} bands (which grow) are assigned to the formation of **1B** (Scheme 2, step 2) based on spectra of genuine product (see Experimental Section).

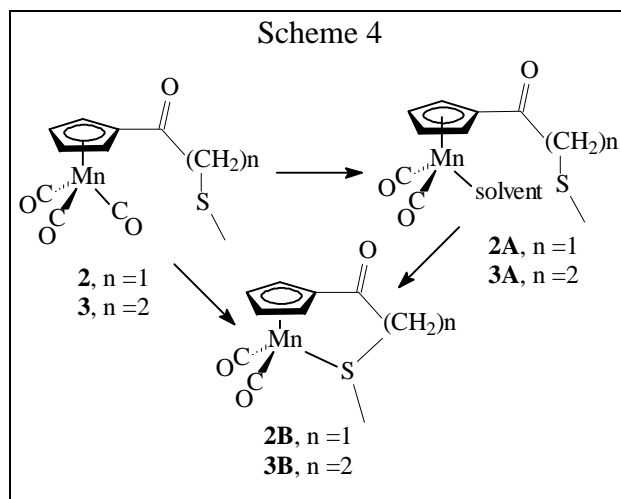
The displacement of CO by solvent clearly must contribute to ϕ_1 , but we propose that reaction with THT must also contribute to ϕ_1 at higher THT concentrations. If a fraction of the metal complex reacts with THT faster than the transducer time scale at high THT concentration then heat from this reaction will contribute to ϕ_1 . This leaves less complex to react at slower times, and thus the contribution to ϕ_2 is less at high THT concentrations. This explanation accounts for the opposing trends observed for ϕ_1 and ϕ_2 in experiments with **1**. The extrapolation of ϕ_1 and ϕ_2 to zero ligand concentration should provide values for ϕ_1 and ϕ_2 that respectively correspond only to CO displacement by solvent (Scheme 3, first step) and solvent displacement by ligand (Scheme 3, second step). Reaction of **1A** with unphotolyzed **1** (*ca* 75 μ M) is not likely to contribute to ϕ_2 since this would require a bimolecular rate constant greater than $10^{10} \text{ M}^{-1} \text{ s}^{-1}$.

The constant value for the sum of ϕ_1 and ϕ_2 indicates that the quantum yield for the overall reaction must be constant (see eq 1 and 2). At high THT concentration, occasionally THT might be expected to be in the solvent cage and react with the metal center immediately following UV photolysis. If this were the case, we would have expected the quantum yield to have increased with THT concentration. Thus the invariance of the quantum yield at the highest THT concentrations used suggests that THT does not react with the metal center prior to solvent coordination. This conclusion is confirmed by the absence of product IR bands at a 200 ps time delay (measured at 0.36 M THT).

The bimolecular rate constants for the reactions of **1A** are the slowest that have been reported for alkane solvent displacement. For example, the reaction of $(\text{C}_5\text{H}_5)\text{Mn}(\text{CO})_2(\text{heptane})$ with THF $(4.4 \pm 0.4 \times 10^6 \text{ M}^{-1} \text{ s}^{-1})^{18}$ is an order of magnitude faster than the reaction of $(\text{C}_5\text{H}_4\text{COCH}_3)\text{Mn}(\text{CO})_2(\text{heptane})$ with THF. Similarly, $\text{W}(\text{CO})_5(\text{heptane})$ and $\text{Mo}(\text{CO})_5(\text{heptane})$ respectively react with rate constants one and two orders of magnitude larger.¹⁹ The results suggest that this Mn-heptane bond is one of the strongest metal-alkane bonds studied to date.²⁰ The energetic data ($\Delta H_1 + \Delta H_2$) also

indicate that the magnitude of Mn-L bond energies are in the order of CO > THT > OP(OEt)₃ > THF > heptane.

The IR experiments demonstrate that ring-closed (**2B**) and solvent-coordinated (**2A**) complexes are both formed in less than 200 ps after photolysis of **2** and that **2A** is converted into **2B** in about 30 ns (Scheme 4). The bands at 1906 and 1968 cm⁻¹ are assigned to **2A** by analogy to the assignments for **1A**. The bands at 1958 and 1898 cm⁻¹ are assigned to **2B** by comparison with spectra



of genuine product.⁸ On the ns time scale, the **2A** bands decay to the same extent that those for **2B** bands increase. Since no other bands appear we conclude that the ring closure of **2A** displaces solvent to form **2B**. The constant total intensity of the **2A** (1898 cm⁻¹) and **2B** (1906 cm⁻¹) bands implies that the peak extinction coefficients for these bands are the same. In general, the band intensities can be used to calculate the ratio of product to transient species at a 200 ps delay yielding 0:1 for **1**, 1:1 for **2**, and 1:3 for **3** (see Table 2).

The total heat ($\Delta H_1 + \Delta H_2$) released after photolysis of **2** is the same as that for **1** reacting with THT, thus the same overall reaction (substitution of CO by S) occurs in each PAC experiment. Since no ϕ_2 is detected for **2** and all the heat was released in a single decay (ϕ_1) we further conclude that the ring closure for **2** is much faster than the response of the PAC experiment ($k > 10^7 \text{ s}^{-1}$), a conclusion consistent with the IR results.

The appearance of a solvent coordinated complex (**2A**) was not anticipated in light of the unit quantum yield reported for ring closure.⁴ If every photon leads to product then no CO recombination

can occur. The simplest explanation is that CO recombination cannot compete with ring closure, and we previously concluded that ring closure is faster than CO recombination.⁴ The ring closure would have to be extremely fast since geminate CO recombination has been reported to be about 300 fs for other metal carbonyls.³ We expected that the formation of the metal-alkane bond would be slower than the formation of the metal-CO bond since a metal-alkane bond is much weaker than a metal-CO bond and the excess energy of the metal fragment would be a greater hindrance to the formation of the weaker bond.²¹ Nevertheless our IR data show that alkane solvent coordination does compete with ring closure suggesting that solvent coordination is also *faster* than CO recombination. We cannot rule out the possibility that the side-chain methyl or methylene is coordinated instead of the solvent in **2A**, but solvent coordination seems to be more consistent with the results of conformational analysis (*vide infra*).

The results for **3** are very similar to those for **2**. The bands at 1907 and 1968 cm⁻¹ are assigned to **3A** by analogy to **1A** and **2A** (Scheme 4). The bands at 1958 and 1895 cm⁻¹ are assigned to **3B** by comparison with spectra of genuine product.⁸ The conversion of **3A** to **3B** is about 10 times slower than the conversion of **2A** to **2B**. This is expected since the activation entropy will be greater for closing the larger ring, which has more degrees of freedom.

Two heat decays are observed after photolysis of **3** with ΔH_1 and ΔH_2 values between those reported for **1** and **2**. On the other hand, the sum of the enthalpies is the same as those observed for **1** and **2** indicating that the overall reaction is the same for **1**, **2** and **3**. The rate constant for ϕ_2 is comparable to those assigned to the IR bands of **3A** and **3B**. We assign this ϕ_2 to the ring closure (**3A** to **3B**), but since ΔH_2 is less exothermic than that observed for **1** we conclude (in an analysis similar to that used for **1**) that not all the ring closure is represented by ϕ_2 and some must contribute to ϕ_1 . Consistent with this conclusion the ΔH_1 for **3** is more exothermic than the ΔH_1 for **1** (since some Mn-

S bonds have already formed) but is less exothermic than the ΔH_1 for **2** (since replacement of Mn-solvent by Mn-S is not complete). This is in agreement with the transient IR results where some **3B** is formed immediately ($k > 10^7 \text{ s}^{-1}$).

The constant values for the enthalpies of ligand exchange with THT for **1** and ring closure for **2** and **3** is not surprising considering the same type of bonds are broken and formed in each case. This observation indicates that there is little ring strain in **2** or **3** contrary to conclusions based on spectroscopic studies.⁸ The constant enthalpy also indicates that the contribution to the photoacoustic signal from the molecular volume changes during the reactions are similar for the all three reactions. The reaction of **1** is an intermolecular reaction and is fundamentally different than the intramolecular reactions for **2** and **3**, and the reaction volume changes should be different. Since these differences do not significantly change the calculated overall enthalpies we conclude that the molecular volume changes make a negligible contribution to the photoacoustic signal compared to that from thermal expansion. This conclusion is further supported by results for ligand substitution with $\text{Mo}(\text{CO})_6$ where reaction volumes were shown to have an insignificant contribution to the photoacoustic signal.²²

Conformational analysis based on molecular mechanics calculations indicates that the distribution of products 200 ps after photolysis of **2** and **3** is determined by the preferred conformations. The thiomethyl group for **2** is near the metal center 50% of the time while the thiomethyl group for **3** is near the metal center 25% of the time. This corresponds with the intensity distribution observed by transient IR (see Table 2). These results suggest that once the CO dissociates from the parent species, the metal center immediately reacts with whatever is available. The analysis does not account for the 20% of **3** that is reformed (based on the quantum yield measurements), that is, the distribution following photolysis is actually ~~4:3~~1:3:1 for **3:3A:3B**. We

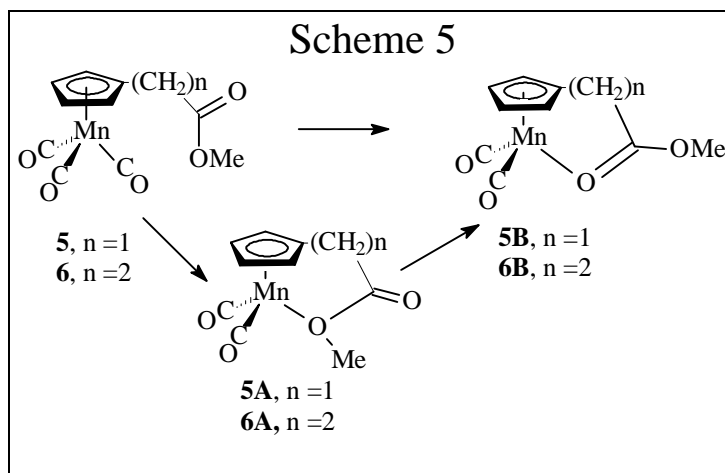
believe that the residual **3** is due to recombination of CO and not deactivation of the excited state prior to CO dissociation since no excited state deactivation occurs for **2**.

What is not clear from this analysis is why **2** does not allow CO recombination but **3** does. There must be a point along the reaction coordinate where there is a vacant site at the metal and CO is in the solvent cage. Once solvent coordination occurs, displacement of solvent by CO is slow and is governed largely by the rate of solvent dissociation.²³ Thus solvent coordination forces CO to diffuse out of the solvent cage. The displacement of solvent by CO must now compete with the “slow ring closure”. Even if all the complex is photolyzed the concentration of CO is no more than 4 mM, and the first-order rate constant will only be about 10^3 s^{-1} . This cannot compete with the slow (10^6 s^{-1}) ring closure of **3**. Even if CO reenters the solvent cage in a secondary geminate recombination it is still destined to diffuse away.²⁴ We conclude that non-geminate recombination of CO cannot compete with ring closure of **2** or **3**.

Examination of PAC data for **4** suggest that the quantum yield we previously reported for **4** may be in error and should be investigated further. Two results for **4** are inconsistent with those of the other complexes. First, the structure of **4** is similar to **1** and **3** yet the quantum yield for **4** is different. Second, and more significant, the ΔH_1 for **4** is much more endothermic than the ΔH_1 for **1**. Ring closure, if it occurs, would make ΔH_1 for **4** more exothermic than for **1** not less. If no ring closure occurs for **4**, ΔH_1 should be the same for **1** since the Mn-CO bond and Mn-solvent bonds strengths should be the similar in both cases. Indeed, if we assume the quantum yield for **4** is the same as it is for **1** and **3** then the ΔH_1 for **4** is the same as it is for **1** (see second entry for **4** in Table 1). With this assumption the results suggest that no ring closure occurs for **4** during the first heat decay, or if it does, the enthalpy of ring closure is the same as for solvent coordination. The latter possibility is inconsistent with the exothermic second heat decay observed for **1** with THF and for **4**.

The second heat decay for **4** is most likely due to ring closure by analogy to the results for **2** and **3**. This ring closure is slower than that for **2** even though the number of ring atoms in each case is the same. The shorter bond lengths associated with oxygen versus sulfur probably results in a ring strain that increases the barrier to ring closure. Ring strain would also account for the less exothermic ΔH_2 for the ring closure of **4** compared to the ligand substitution of **1** with THF.

The unit quantum yield for **5** suggests a rapid ring closure like that observed for **2**,⁴ yet a second heat decay was detected indicating a relatively slow process. We propose that ring closure is rapid but that there are two modes of ring closure (Scheme 5). Both side-chain



oxygens can initially bond with the metal, but the complex with the less stable Mn-O ether bond rearranges to the one with the more stable Mn-O carbonyl bond. An analogous mechanism explains the results for **6**.

Summary

Extremely fast ring closures have been observed for $(\eta^5\text{-C}_5\text{H}_4\text{R})\text{Mn}(\text{CO})_3$ complexes; in addition, the ring closure can occur via two pathways of distinct time scales. The first pathway is an ultrafast ring closure following CO dissociation that occurs prior to solvent coordination. The second pathway is a ns- μ s ring closure that displaces coordinated solvent. Rapid ring closure and high quantum yields are determined by favorable side chain conformations.

Supporting Information Available: Descriptions of the syntheses of **1**, **2** and **3**, and tables of PAC data for **1-6**. See any current masthead page for ordering information and Web access instructions.

Acknowledgments

The Donors of the Petroleum Research Fund, administered by the American Chemical Society, and a University of Memphis Faculty Research Grant are acknowledged for partial support of this research.

-
- 1 Wieland, S.; van Eldik, R. *J. Phys. Chem.*, **1990**, 94, 5865.
 - 2 Burdett, J. K.; Grzybowski, J. M.; Perutz, R. N.; Poliakoff, M.; Turner, J. J.; Turner, R. F. *Inorg. Chem.* **1978**, 17, 147. (b) Turner, J. J.; Poliakoff, M. *ACS Symp. Ser.* **1983**, 200, 35.
 - 3 Kim, S. K.; Pedersen, S.; Zewail, A. H. *Chem. Phys. Lett.* **1995**, 233, 500. (b) Schwartz, B. J. King, J. C.; Zhang, J. Z.; Harris, C. B. *Chem. Phys. Lett.* **1993**, 203, 503.
 - 4 Pang, Z.; Burkey, T. J.; Johnston, R. F. *Organometallics* **1997**, 16, 120.
 - 5 (a) Sorenson, A. A.; Yang, G. K. *J. Am. Chem. Soc.* **1991**, 113, 7061. (b) Winnik, M. A. *Chem. Rev.* **1981**, 81, 491. (b) Scott, T. W.; Doubleday, Jr. C. *Chem. Phys. Lett.* **1991**, 178, 9.
 - 6 For a notable exception see the following paper: Zhang, J. Z.; Schwartz, B. J.; King, J. C.; Harris, C. B. *J. Am. Chem. Soc.* **1992**, 114, 10921.
 - 7 Certain commercial equipment, instruments, or materials are identified in this paper in order to adequately specify the experimental procedure. In no case does such identification imply recommendation or endorsement by NIST, nor does it imply that the materials or equipment identified are necessarily the best available for the purpose.
 - 8 Pang, Z.; Johnston, R. F.; VanDerveer, D. G. *J. Organomet. Chem.* **1996**, 526, 25.
 - 9 Yeh, P.-H.; Pang, Z.; Johnston, R. F. *J. Organometal. Chem.* **1996**, 509, 123.
 - 10 Nayak, S. K.; Burkey, T. J. *Organometallics* **1991**, 10, 3745.
 - 11 Leu, G.-L.; Burkey, T. J. *J. Coord. Chem.* **1995**, 34, 87.
 - 12 Maciejewski, A.; Jaworska-Augustyniak, A.; Szeluga, Z.; Wojtczak, J.; Karolczak, J. *Chem. Phys. Lett.*, **1988**, 153, 227.
 - 13 Dougherty, T. P. and Heilweil, E. J. *Optics Letters* **1994**, 19, 129.
 - 14 Arrivo, S. M.; Kleiman, V. D.; Dougherty, T. P. and Heilweil, E. J. *Optics Letters* **1997**, 22, 1488.

-
- 15 At time delays less than 200 ps the metal carbonyl molecules are still vibrationally excited and the individual IR absorbance bands are not well resolved.
- 16 In additional PAC experiments for **3** in *n*-hexane we obtained $k = (1.26 \pm 0.14) \times 10^6 \text{ s}^{-1}$. Although the PAC and IR experiments were done in different solvents this apparently is only responsible for a minor change in the rate. Differences in rates obtained by PAC and IR experiments are attributed to the fact that IR experiments were not air free.
- 17 Creaven, B. S.; Dixon, A. J.; Kelly, J. M.; Long, C.; Poliakoff, M. *Organometallics* **1987**, 6, 2600.
- 18 Yang, P.-F.; Yang, G. K. *J. Am. Chem. Soc.* **1992**, 114, 6937.
- 19 Burney, D. P. Ph. D. Thesis, The University of Memphis, 1994.
- 20 Burkey, T. J. *J. Am. Chem. Soc.* **1990**, 112, 8239.
- 21 King, J. C.; Zhang, J. Z.; Schwartz, B. J.; Harris, C. B. *J. Chem. Phys.* **1993**, 99, 7595.
- 22 Jiao, T.; Leu, G. L.; Farrell, G.; Burkey, T. J. unpublished results.
- 23 $k = 3 \times 10^5 \text{ M}^{-1} \text{ s}^{-1}$ for R = H, and our data show that rates are even slower for solvent displacement for R = COCH₃, see reference 17.
- 24 For further discussion of the fate of caged CO see reference 10.